Progress In Electromagnetics Research Letters, Vol. 92, 61–67, 2020

Ultra-Compact Bandpass Filter with Super Wide Upper Stopband

Yang Xiong[1], Wei Zhang[2], and Li-Tian Wang[3, *]

Abstract—An S-band bandpass filter based on quarter wavelength stepped-impedance resonators (SIRs) is presented in this paper. Two SIRs are loaded to the BPF to obtain wide stopband suppression. The center frequency f_0 of the bandpass filter is located at 2.105 GHz with 3-dB fraction bandwidth (FBW) of 11.9%. It shows that the spurs free upper stopband with 15 dB rejection level can extend to 40 GHz ($19f_0$). The circuit size of this filter is extremely compact, which occupies only 7.35 mm×7.5 mm.

1. INTRODUCTION

Recently, microwave bandpass filters (BPFs) with compact size, high selectivity, and harmonic suppression have aroused wide concern. The inherent spurs and harmonics in out-of-band due to the periodic characteristic of transmission line make the filters hard to be applied in RF front-end. Various practical and effective approaches focused on harmonic suppression are presented [1–12]. It is convenient to design a BPF with wide stopband by cascading a lowpass filter and a highpass filter [1], but it usually occupies larger circuit area. Defected ground structure (DGS) technology is widely used to suppress the harmonic responses due to the good lowpass characteristics [2, 3]. Generally, DGS can provide harmonic suppression in upper stopband and reduce the circuit area. However, the fabrication of a DGS filter is complicated, and it is difficult to integrate with planar circuits. The method of using stepped-impedance resonators (SIRs) to push the harmonic frequencies to higher frequencies by adjusting the ratio of impedance has been demonstrated for the design of wide upper stopband BPFs [4–6, 10]. Besides, harmonics-staggered filters [7, 8], defected microstrip structures [9, 10], and infused spur-lines [11, 12] are popularly used to suppress the unwanted harmonic passbands. Although the merits of these filters have been fully demonstrated, the spurs-like responses in out-of-band should be further improved.

In this letter, we present an ultra-compact S-band BPF with super wide spurs free upper stopband. The filter consists of two cascaded quarter wavelength SIRs. By loading SIRs, transmission zeros are generated to suppress the out-of-band spurs. The method for spurious suppression is very simple and effective, while it does not increase the complexity of fabrication and circuit size at all. For experimental validation, the filter is designed, fabricated, and tested. The measurement results show that the center frequency f_0 is located at 2.105 GHz with 3-dB fraction bandwidth (FBW) of 11.9%. Its upper stopband with 15 dB rejection level can extend to 40 GHz ($19f_0$). The fabricated filter occupies very compact size of 7.35 mm × 7.5 mm.

2. BPF ANALYSIS AND DESIGN

The configuration and coupling topology of the proposed S-band BPF, respectively, are depicted in Figs. 1(a) and 1(b). It is shown that the BPF consists of two cascaded quarter wavelength SIRs. As

Received 6 November 2019, Accepted 27 April 2020, Scheduled 22 June 2020

* Corresponding author: Li-Tian Wang (wanglitianrf@sina.com).

[1] Southwest China Institute of Electronic Technology, Chengdu 610036, China. [2] Chongqing Acoustic-Optic-Electronic Company, China Electronics Technology Group Corporation, Chongqing 400060, China. [3] College of Electronic Information and Optical Engineering, Nankai University, Tianjin 300350, China.

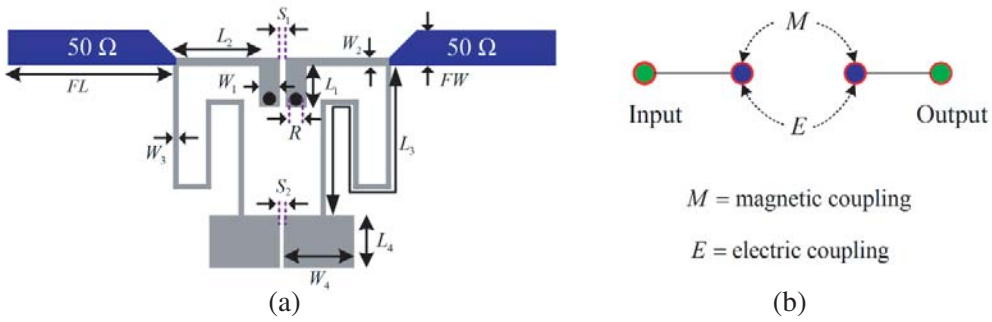

Figure 1. (a) Configuration of BPF, (b) coupling topology.

shown in Fig. 1(a), L_k and W_k ($k = 1, 2, 3, 4$) denote the physical length and width of the resonator, respectively. S_1 and S_2, respectively, are the gaps of two shorted coupling lines and two open coupling lines. R represents the diameter of the via holes. As shown in Fig. 1(b), mixed electric and magnetic coupling is introduced, in which the shorted coupling lines provide magnetic coupling, and the open coupling lines provide electric coupling.

Figure 2(a) shows the configuration of a quarter wavelength SIR. According to transmission line theory:

$$\begin{bmatrix} A & B \\ C & D \end{bmatrix} = M_2 M_1 \tag{1}$$

where,

$$M_2 = \begin{bmatrix} \cos\theta_2 & \mathrm{j}\sin\theta_2 Z_2 \\ \mathrm{j}\sin\theta_2/Z_2 & \cos\theta_2 \end{bmatrix} \tag{2}$$

$$M_1 = \begin{bmatrix} \cos\theta_1 & \mathrm{j}\sin\theta_1 Z_1 \\ \mathrm{j}\sin\theta_1/Z_1 & \cos\theta_1 \end{bmatrix} \tag{3}$$

Here, Z_2 and θ_2 denote the characteristic impedance and electrical length of low-impedance transmission line. Z_1 and θ_1 represent the characteristic impedance and electrical length of high-impedance transmission line.

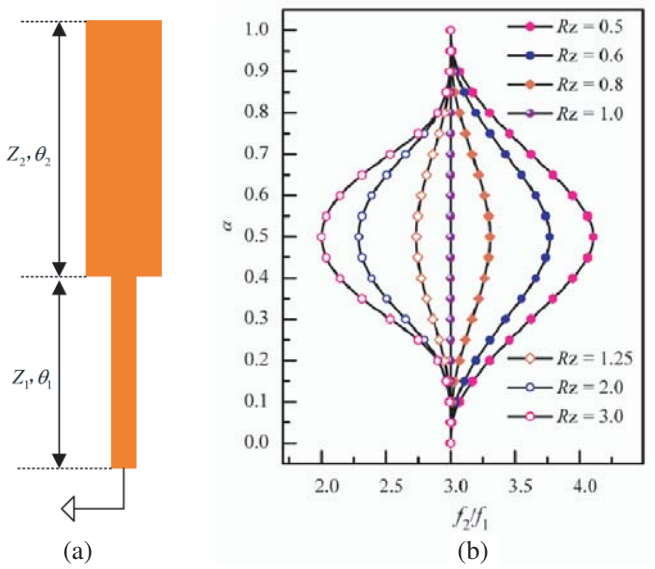

Figure 2. (a) Configuration of quarter wavelength SIR, (b) the relationship between f_2/f_1 and α under different R_Z.

Therefore, the input impedance Z_{in} of quarter wavelength SIR can be expressed as:

$$Z_{in} = \frac{AZ_L + B}{CZ_L + D} \tag{4}$$

Here, $Z_L = 0$. According to the resonant condition of $Y_{in} = 0$ [13–15], we have

$$Y_{in} = \frac{D}{B} = -\frac{j}{Z_2}\frac{Z_2 - Z_1 \tan\theta_1 \tan\theta_2}{Z_1 \tan\theta_1 + Z_2 \tan\theta_2} = 0 \tag{5}$$

$$\tan\theta_1 \tan\theta_2 = Z_2/Z_1 = R_Z \tag{6}$$

where Y_{in} denotes the input admittance of quarter wavelength SIR, and R_Z is the impedance ratio.

Therefore, the resonant modes f_1 and f_2 (the fundamental resonant frequency and the first harmonic resonant frequency) of the quarter wavelength SIR can be derived by solving Eq. (6).

Here, we define the ratio of electrical length α as

$$\alpha = \frac{\theta_1}{\theta_1 + \theta_2} \tag{7}$$

under the condition of $\theta_1 + \theta_2 = \pi/2$.

Figure 2(b) shows the relationship between f_2/f_1 and α under different R_Z. It can be found that quarter wavelength SIR is of harmonic suppression when R_Z is less than 1. Fig. 3(a) plots the diagram of the normalized first and second harmonic resonant frequencies (f_2/f_1 and f_3/f_1) against α under different R_Z. The ratio of normalized second and first harmonic resonant frequencies is depicted in Fig. 3(b).

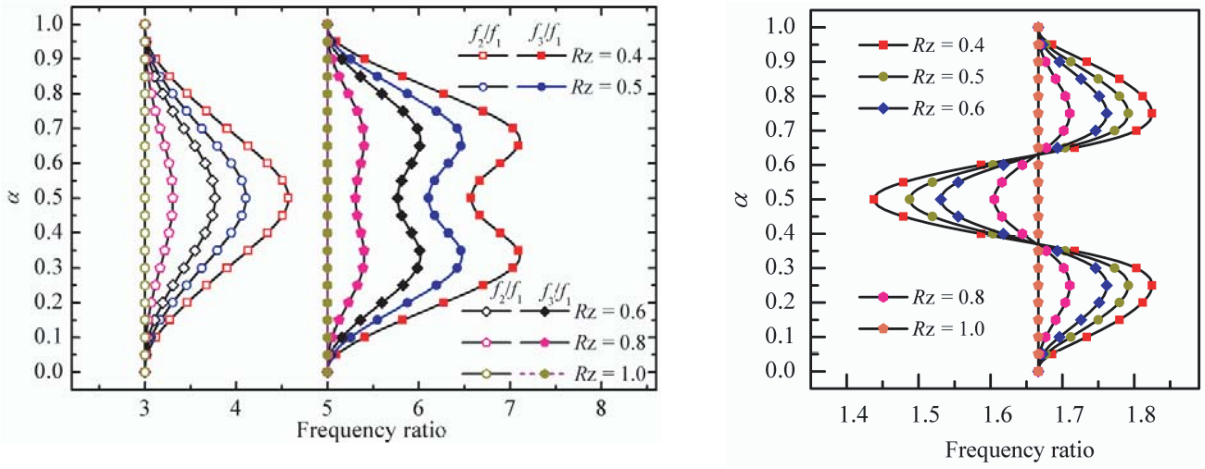

Figure 3. (a) The normalized first and second harmonic resonant frequency against α under different R_Z, (b) f_3/f_2 versus varied α under differentR_Z.

According to [16], the coupling coefficient can be extracted as:

$$M_{12} = \frac{f_2^2 - f_1^2}{f_2^2 + f_1^2} \tag{8}$$

Figure 4(a) plots the extracted coupling coefficient M_{12} versus varied L_1 and S_2. As can be seen, the coupling coefficient decreases as S_2 increases from 0.07 mm to 0.27 mm, when L_1 is fixed. The coupling coefficient decreases slightly as L_1 gets larger, when S_2 is fixed. The extracted coupling coefficient M_{12} versus varied S_1 and S_2 is depicted in Fig. 4(b). It shows that the coupling coefficient decreases as S_2 increases from 0.05 mm to 0.45 mm, when S_1 is fixed. However, the coupling coefficient keeps almost unchanged as S_1 becomes larger, when S_2 is fixed.

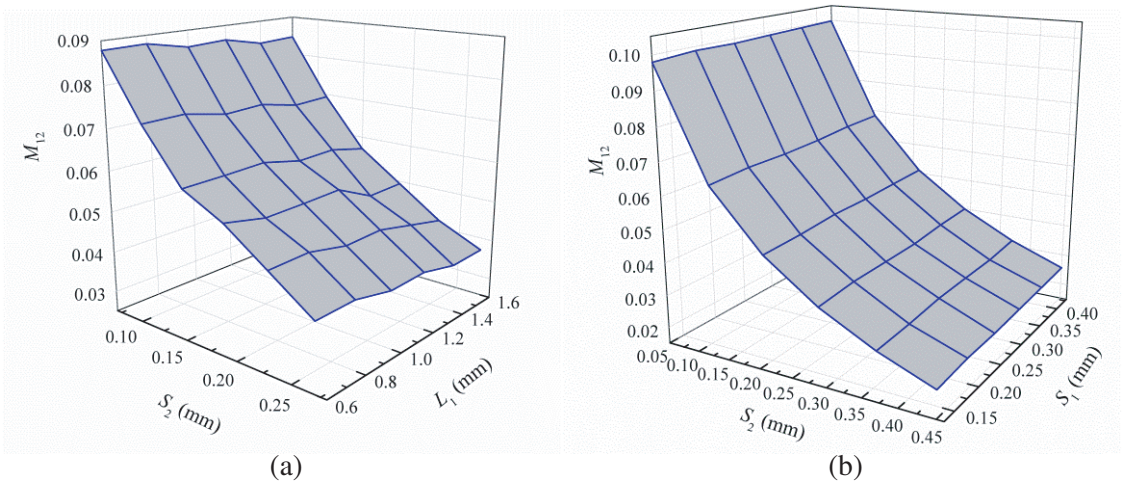

Figure 4. Coupling coefficient M_{12} versus varied (a) L_1 and S_2, (b) S_1 and S_2.

Next, the external quality factor Q_e can be derived by [16]:

$$Q_e = \frac{\omega_0 \tau_{S_{11}}(\omega_0)}{4} \tag{9}$$

where ω_0 denotes the resonant frequency, and $\tau_{S_{11}}(\omega_0)$ is the group delay of S_{11} at ω_0.

Figure 5 shows the relationship between the extracted external quality factor Q_e and the tap position t. As expected, with the increase of t, the coupling strength becomes larger.

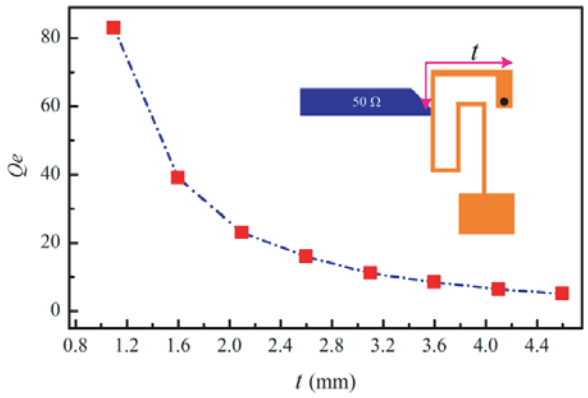

Figure 5. The external quality factor Q_e versus varied t.

Due to the periodic characteristic of transmission line, the inherent spurs and harmonics in out-of-band usually make the filters hard to be applied in RF front-end. Therefore, the harmonic frequencies in upper stopband should be further suppressed. In this letter, two SIRs are loaded to the original BPF to suppress the harmonics. Fig. 6(a) plots the layout of the modified BPF.

Figure 6(b) shows the frequency responses of BPF with and without SIRs loaded. It can be found that the out-of-band performance has been improved with SIRs loaded, whereas the passband keeps almost unchanged.

3. EXPERIMENTAL RESULTS AND DISCUSSION

In order to validate the analysis above, BPF with SIRs loaded is finally printed on a substrate of Rogers 4003C, with thickness of $h = 0.508$ mm and relative dielectric constant of $\varepsilon_r = 3.55$. The circuit

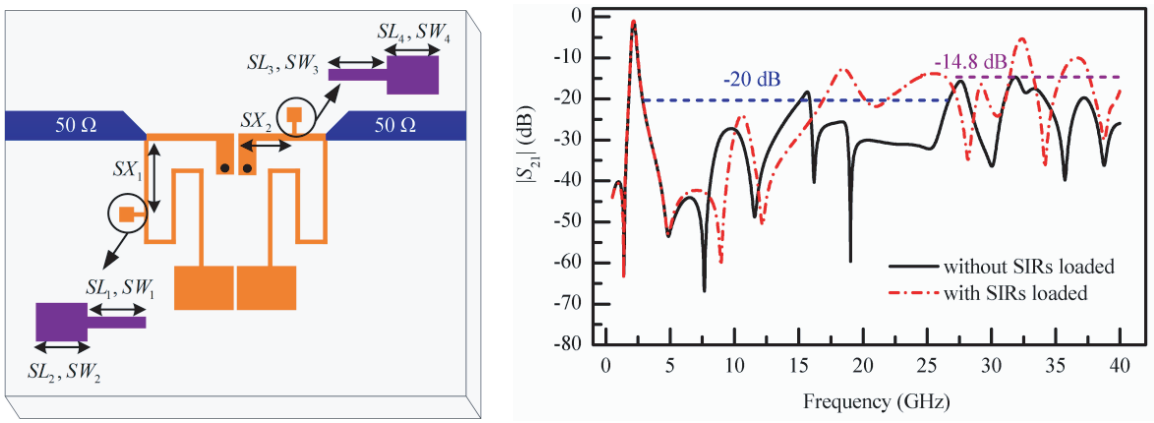

(a) (b)

Figure 6. (a) Layout of BPF with two SIRs loaded, (b) simulation results with and without SIRs loaded.

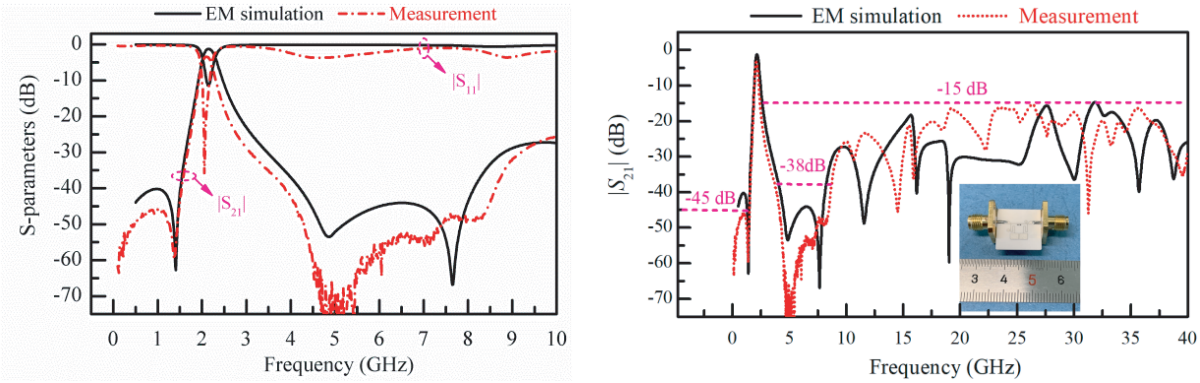

(a) (b)

Figure 7. (a) Local frequency range responses, (b) wideband band frequency responses of $|S_{21}|$.

Table 1. Comparison with previous reported works.

Ref.	f_0 (GHz)	3-dB FBW (%)	RL (dB)	Stopband suppression	Circuit area ($\lambda_g \times \lambda_g$)
[3]	2.0	26	> 10	$6f_0$ (24 dB)	0.23×0.12
[5]	2.4	10.3	> 12	$4.36f_0$ (20 dB)	0.472×0.256
[6]	0.35	13.7	> 14	$6.86f_0$ (19.4 dB)	0.064×0.062
[10]	2.35	6.79	> 20	$5.64f_0$ (21.9 dB)	0.438×0.301
[11]	0.38	48.5	17.5	$8.7f_0$ (25 dB)	0.12×0.09
[12]	2.45	12.5	18	$4f_0$ (20 dB)	0.13×0.12
This work	**2.105**	**11.9**	**35.8**	$\mathbf{19}f_0$ **(15 dB)**	$\mathbf{0.088 \times 0.086}$

dimensions of the proposed BPF are given as (all in millimeter): $L_1 = 1.0$, $L_2 = 2.3$, $L_3 = 9.8$, $L_4 = 2.3$, $SL_1 = 0.4$, $SL_2 = 0.8$, $SL_3 = 0.4$, $SL_4 = 0.8$, $W_1 = 0.6$, $W_2 = 0.2$, $W_3 = 0.1$, $W_4 = 3$, $SW_1 = 0.2$, $SW_2 = 0.8$, $SW_3 = 0.2$, $SW_4 = 0.8$, $S_1 = 0.25$, $S_2 = 0.1$, $FL = 5$, $FW = 1.175$, $SX_1 = 2.5$, $SX_2 = 1.8$, $R = 0.3$, $t = 2.9$. The overall size of the filter occupies only 7.35 mm × 7.55 mm (excluding feeding lines). This corresponds to $0.086\lambda_g \times 0.088\lambda_g$, where λ_g is the guided wavelength of a 50 Ω microstrip

line at f_0. Agilent vector network analyzer N5244A is used to characterize the frequency responses of BPF. As shown in Fig. 7, the measurement results are in good agreement with the prediction ones. It can be observed from Figs. 7(a) and 7(b) that the center frequency f_0 is located at 2.105 GHz with 3-dB FBW of 11.9%. The measured return loss (RL) within the passband is greater than 35.8 dB. As can be seen, the lower stopband suppression can reach 45 dB from DC to 1.48 GHz, while the upper stopband with rejection level of 15 dB can extend to 40 GHz. Table 1 summarizes the comparison between this work and other reported BPFs, which shows that the proposed BPF is of very compact size, super wide upper stopband, and good in-band RL.

4. CONCLUSION

An S-band BPF with compact size, wide upper stopband, and good in-band RL based on quarter wavelength stepped-impedance resonators (SIRs) is presented in this paper. Mixed electric and magnetic coupling is introduced in this design. To suppress the spurs in out-of-band, two SIRs are loaded to the original BPF. It shows that the modified BPF is of super wide upper stopband, whose 15 dB rejection level can extend to 40 GHz ($19f_0$). The circuit size of the filter is extremely compact, which occupies only 7.35 mm $\times$ 7.5 mm.

REFERENCES

1. Xu, J., Y.-X. Ji, W. Wu, and C. Miao, "Design of miniaturized microstrip LPF and wideband BPF with ultra-wide stopband," *IEEE Microwave and Wireless Components Letters*, Vol. 23, No. 8, 397–399, 2013.
2. Peng, B., S. Li, J. F. Zhu, Q. Y. Zhang, L. Deng, Q. S. Zeng, and Y. Gao, "Wideband bandpass filter with high selectivity based on dual-mode DGS resonator," *Microwave and Optical Technology Letters*, Vol. 58, No. 1, 2300–2303, 2016.
3. Peng, B., S. F. Li, B. Zhang, and S. Wang, "Compact multimode bandpass filters with wide upper stopband using dual-mode DGS resonators," *2014 Asia-Pacific Microwave Conference (APMC)*, 4–7, 2014.
4. Kim, C. H. and K. Chang, "Wide-stopband bandpass filters using asymmetric stepped-impedance resonators," *IEEE Microwave and Wireless Components Letters*, Vol. 23, No. 2, 69–71, 2013.
5. Liu, H. W., B. P. Ren, S. Li, X. H. Guan, P. Wen, X. Xiao, and Y. Peng, "High-temperature superconducting bandpass filter using asymmetric stepped-impedance resonators with wide-stopband performance," *IEEE Transactions on Applied Superconductivity*, Vol. 25, No. 5, 1501606, 2015.
6. Singh, V., V. K. Killamsetty, and B. Mukherjee, "Miniaturized bandpass filter with wide stopband using spiral configuration of stepped impedance resonator," *Frequenz*, Vol. 72, No. 9–10, 455–458, 2018.
7. Lin, S. C., P. H. Deng, Y. S. Lin, C. H. Wang, and C. H. Chen, "Wide-stopband microstrip bandpass filters using dissimilar quarter-wavelength stepped-impedance resonators," *IEEE Transactions on Microwave Theory and Techniques*, Vol. 54, No. 3, 1011–1018, 2006.
8. Wu, H. W., S. K. Liu, M. H. Weng, and C.-H. Hung, "Compact microstrip bandpass filter with multispurious suppression," *Progress In Electromagnetics Research*, Vol. 107, 21–30, 2010.
9. He, Z. S., Z. H. Shao, and C. J. You, "Parallel feed bandpass filter with high selectivity and wide stopband," *Electronics Letters*, Vol. 52, No. 10, 844–846, 2016.
10. Liu, H. W., F. Liu, X. H. Guan, B. P. Ren, T. K. Liu, Y. F. Wang, P. Wen, and H. X. Xu, "Wide-stopband superconducting bandpass filter using slitted stepped-impedance resonator and composite spurline structure," *IEEE Transactions on Applied Superconductivity*, Vol. 28, No. 8, 1501508, 2018.
11. Killamsetty, V. K. and B. Mukherjee, "Miniaturised highly selective bandpass filter with very wide stopband using meander coupled lines," *Electronics Letters*, Vol. 53, No. 13, 889–890, 2017.

12. Ma, L., K. Song, C. Zhuge, and Y. Fan, "Compact bandpass filter with wide upper stopband based on spiral-shaped resonators and spur-lines," *Progress In Electromagnetics Research Letters*, Vol. 29, 87–95, 2012.
13. Pozar, D. M., *Microwave Engineering*, John Wiley, 2012.
14. Makimoto, M. and S. Yamashita, *Microwave Resonators and Filters for Wireless Communication*, Springer-Verlag, Berlin Heidelberg, 2001.
15. Lin, S. C., P. H. Deng, Y. S. Lin, C. H. Wang, and C. H. Chen, "Wide-stopband microstrip bandpass filters using dissimilar quarter-wavelength stepped-impedance resonators," *IEEE Transactions on Microwave Theory and Techniques*, Vol. 54, No. 3, 1011–1018, 2006.
16. Hong, J. S. and M. J. Lancaster, *Microstrip Filters for RF/Microwave Applications*, Wiley, New York, NY, USA, 2001.